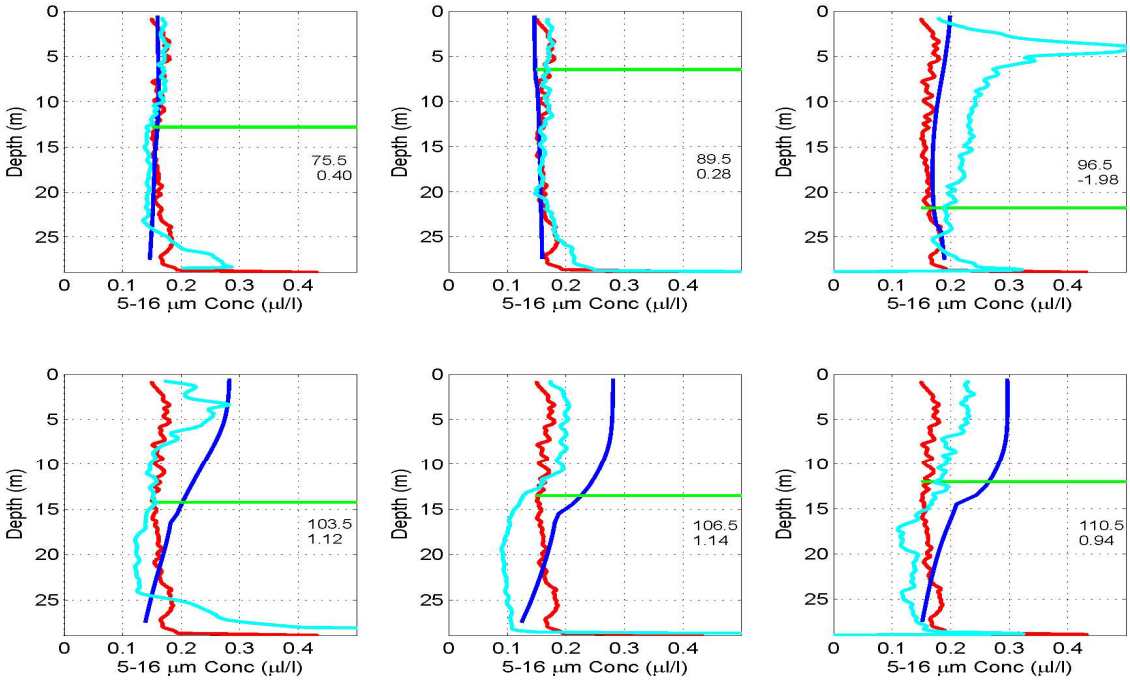


**Figure 2. 22.** SWA particle concentrations predicted by the model (blue) compared to observed concentrations (cyan), which combined 5 μm and 16 μm particles; results include upwelling effects. Initial concentrations are represented by the red line, the green line is the STL depth, and sample day and $W_N$ are on the right.

2.4.2.1 Influence of Upwelling at SWA

Because SWA is located very close to the end of the lake, upwelling and horizontal transport will have a significant effect on the phytoplankton population. During upwelling, bottom water is upwelled to the surface, turned around and transported downwind (Monisimth, 1986). In the model, upwelling and downwind transport was approximated by (2.19), which improved model results but provided less conclusive results than those at NOA and MWY. With (2.19), the model over-predicted concentrations in the STL up to a factor of 1.5 (except for JD 96.5; Figure 2. 22); however, without (2.19) the model over-predicted concentrations up to a factor of 2.7 (Figure 2. 23). On JD 96.5 near the five meter depth, the sharp phytoplankton peak likely results from phytoplankton blown into SWA; winds were southward previous to JD 96.5 (Figure 1.49) and the model omits horizontal advection and cannot simulate such conditions. Exclusion of upwelling effects infers that the model excludes some effect that inhibits phytoplankton growth at SWA, and inclusion of upwelling effects infers that something like upwelling could be inhibiting or diluting phytoplankton growth. The Cedar River could dilute phytoplankton, but analyses in Section One

suggested the Cedar has a very small effect (about 8%) on hydrodynamic conditions at SWA.

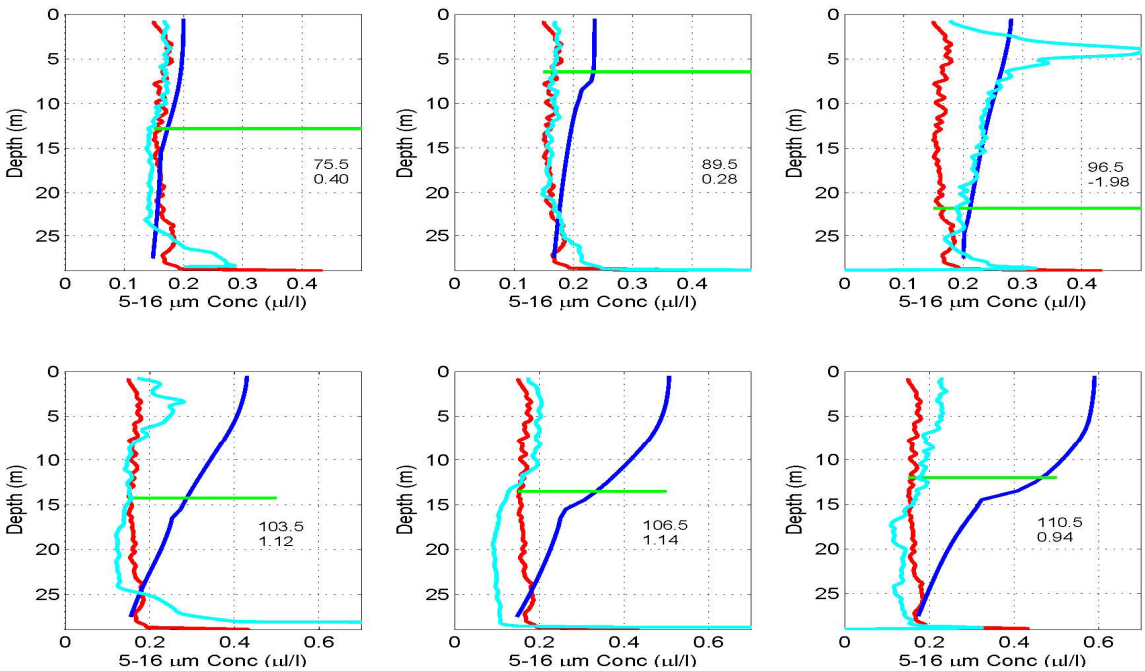


**Figure 2. 23.** SWA particle concentrations predicted without (2.19); the model (blue) compared to observed concentrations (cyan), which combined 5 μm and 16 μm particles; results include upwelling effects. Initial concentrations are represented by the red line, the green line is the STL depth, and sample day and $W_N$ are on the right.

2.4.2.2 Effect of Vertical Eddy Diffusion on Phytoplankton

The model was primarily calibrated to match phytoplankton profiles in the STL and then secondarily to profiles below the STL; model simulations suggest simulated phytoplankton profiles were sensitive to the eddy diffusion profile. Observed phytoplankton concentrations decreased with depth with a concave-upward curvature to the profile in the STL at NOA and MWY but to a lesser degree at SWA; below the STL concentration profiles were more uniform (Figure 2. 20 - Figure 2. 22). More pronounced curvature was obtained when eddy diffusion decayed exponentially in the STL (Figure 2. 24). An exponential decay provided more curvature in the STL (Figure 2. 20) compared to a more step-like profile (Figure 2. 25) and to a uniform profile (Figure 2. 26). While the exponential and step-like profiles used the same general equation (2.27), their difference is in the relative decrease ($\varphi$) in eddy diffusion over the STL depth; setting $K(z)=1.0\times10^{-6}$ $m^2/s$ (diffusion of heat) for $z> h_\psi$ allowed too much growth in the STL. The calibrated $\varphi$

values (Table 2. 14) produced the exponential decay profiles and they are close to the $K_{e(intersect)}/K_{e(surface)}$ ratios in Table 2. 11.

The uniform $K_e$ distribution results suggest phytoplankton growth is unable to overcome diffusive fluxes; the diffusive flux is greater than the net growth rate. For a uniform diffusion profile, Huisman et al. (2002) found phytoplankton blooms can occur when the growth rate exceeds vertical diffusive fluxes, which was defined by a critical eddy diffusion. Based on the uniform profile results presented, the imposed eddy diffusion time series had values greater than Huisman critical eddy diffusion. These results suggest the phytoplankton bloom is sensitive to the vertical distribution of eddy diffusion but is also sensitive to the temporal change in eddy diffusion.

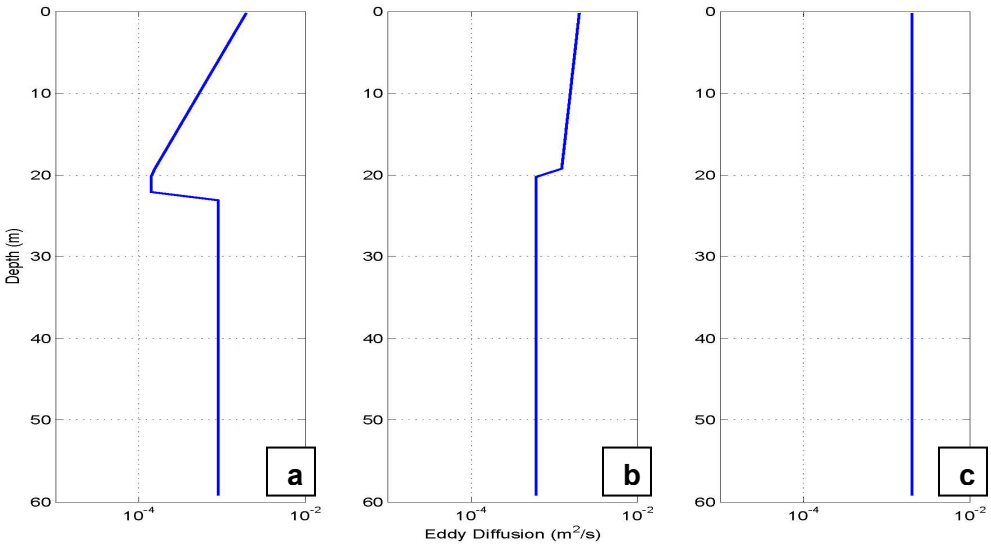


**Figure 2. 24.** Example of eddy diffusion profiles used during model calibration (abscissa is log scale). The STL depth was 20 meters for these profiles. The exponential decay profile in the STL (a) used $\phi$=0.45, $\varphi$=0.07, $\psi$=1.0; the step-like profile used $\phi$=0.3, $\varphi$=0.6, $\psi$=0.5; and the uniform profile used $\phi$=1.0, $\varphi$=1.0, $\psi$=1.0.

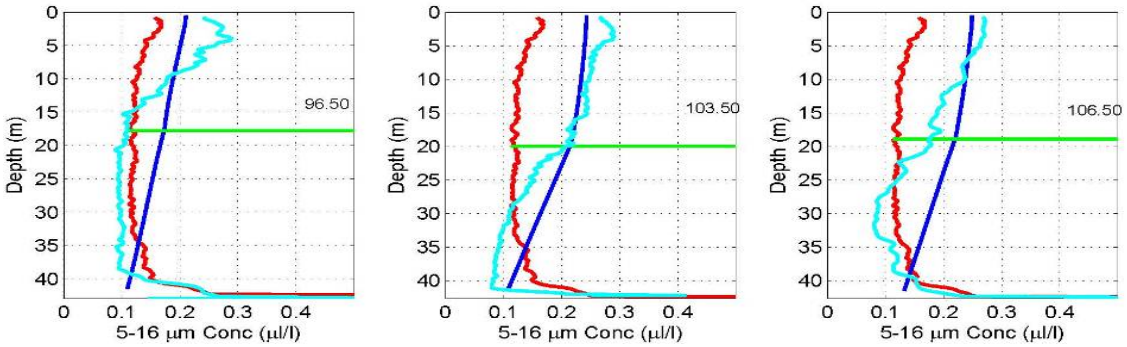


**Figure 2. 25.** NOA particle concentrations using a step profile (blue) with $\phi$=0.3, $\varphi$=0.6, $\psi$=0.5 and $g_{max}$=2.0. Observed concentrations (cyan) combined 5 μm and 16 μm particles. Initial concentrations are represented by the red line, the green line is the STL depth, and sample day is on the right.

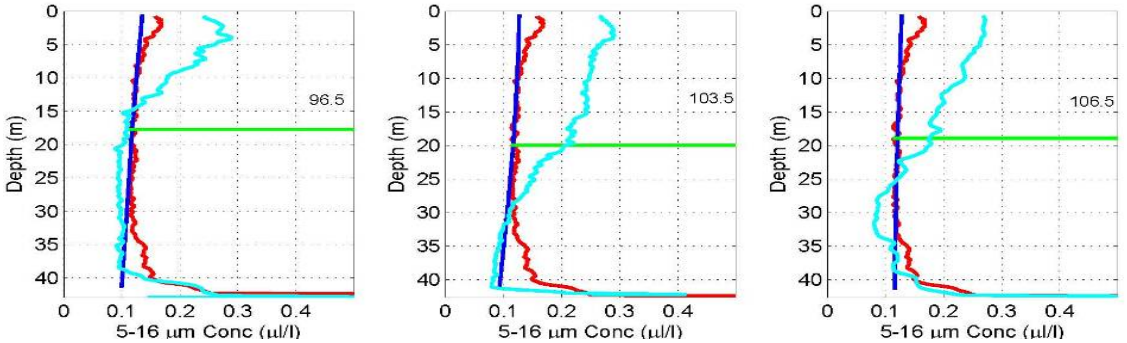


**Figure 2. 26.** NOA particle concentrations using a uniform $K_e$ profile (blue) but with $K_e$ varying temporally; $\phi$=1.0, $\varphi$=1.0, $\psi$=1.0 and $g_{max}$=1.38. Observed concentrations (cyan) combined 5 μm and 16 μm particles. Initial concentrations are represented by the red line, the green line is the STL depth, and sample day is on the right.

The phytoplankton bloom timing or size was also dependent on the temporal change in eddy diffusion. Prior to JD 96.5, eddy diffusion ranged between 0.0002 $m^2/s$ and 0.004 $m^2/s$ but was usually greater than 0.001 $m^2/s$, but near JD 96.5 eddy diffusion decreased about an order of magnitude and persisted to around JD 106.5 (Table 2. 10). During this drop in eddy diffusion, *A. subarctica* and *S. niagarae* population correspondingly increased at MWY and SWA but less so at NOA (Figure 2. 27). Modeling suggests phytoplankton dynamics were sensitive to the temporal change in eddy diffusion. For a temporally constant eddy diffusion, the bloom was significantly repressed for $K_e$=0.004 $m^2/s$ (Figure 2. 28) but substantially enhanced for $K_e$=0.0002 $m^2/s$ (Figure 2. 29). Considering these results with the previous findings for the diffusion profiles, the combined findings suggest the vertical and temporal distributions of eddy diffusion have a significant influence on the timing and size of the phytoplankton bloom. The temporal relaxation of eddy diffusion and its

attenuation with depth presented a condition where the growth rate in the euphotic zone exceeded the diffusive flux out of the euphotic zone.

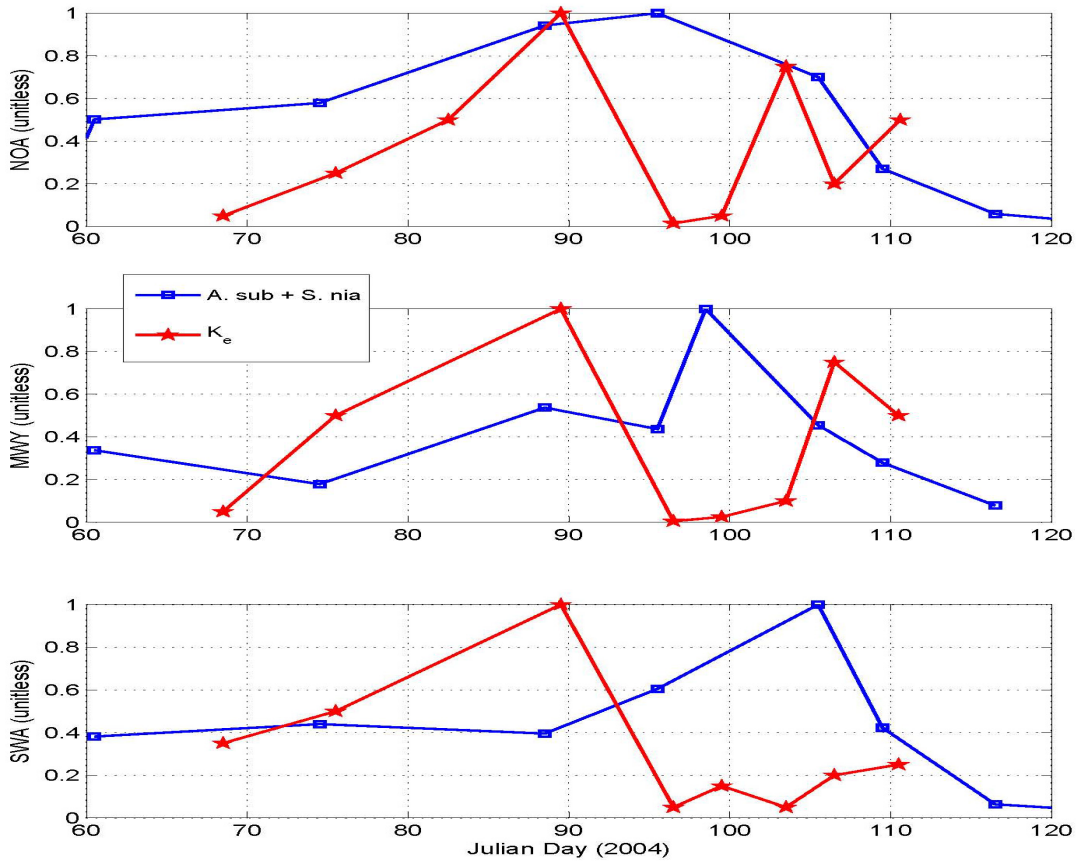


**Figure 2. 27.** Normalized *A. subarctica* and *S. niagarae* (☐) biovolume concentrations and observed eddy diffusion (★). All observations were normalized for better presentation of relative changes between phytoplankton response and eddy diffusion.

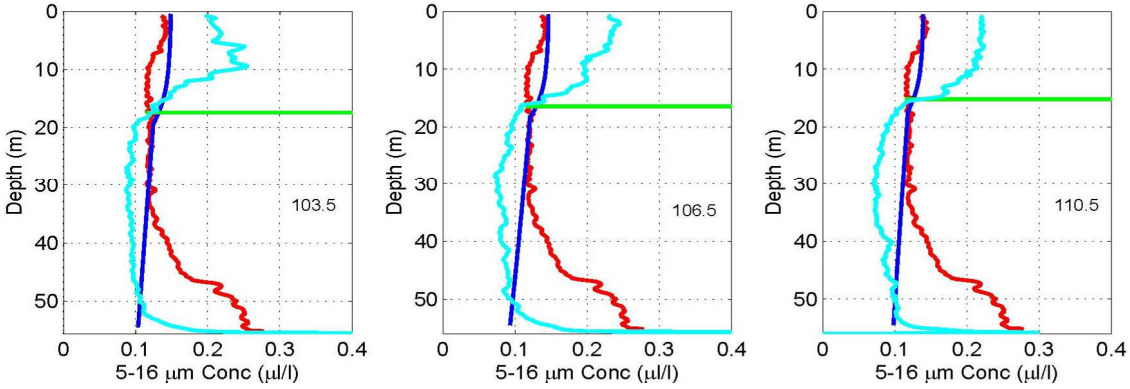


**Figure 2. 28.** MWY particle concentrations for a temporally constant $K_e$=0.004 $m^2$/s (blue) compared to observed concentrations (cyan), which combined 5 μm and 16 μm particles. Initial concentrations are represented by the red line, the green line is the STL depth, and sample day is on the right. $K_e$ varied with depth with $\phi$=0.45, $\varphi$=0.07, and $\psi$=1.0.

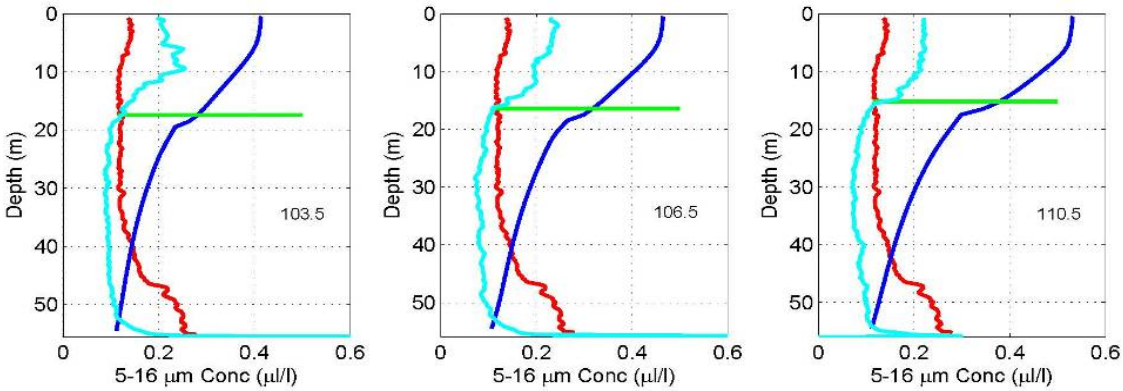


**Figure 2. 29.** MWY particle concentrations for a temporally constant $K_e$=0.0002 $m^2$/s (blue) compared to observed concentrations (cyan), which combined 5 μm and 16 μm particles. Initial concentrations are represented by the red line, the green line is the STL depth, and sample day is on the right. $K_e$ varied with depth defined by $\phi$=0.45, $\varphi$=0.07, and $\psi$=1.0.

Eddy diffusion has a significant influence on the timing and size of the phytoplankton bloom, but incident light is also important. If incident light controls the bloom, then the modeled growth rate should be independent of changes in eddy diffusion. If eddy diffusion controls the bloom, the modeled growth rate should change with eddy diffusion. To test the influence of incident light, three eddy diffusion time series were compared. The first series is the observed series, the second series imposes a constant eddy diffusion of 0.002 $m^2$/s for times after the peak eddy diffusion (0.004 $m^2$/s), and the third series imposes a constant eddy diffusion of 0.004 $m^2$/s. The second series significantly reduced the growth rate after JD 89.5 compared to the first series (Figure 2. 30). The third series produced a negative growth rate after JD 89.5, but prior to JD 89.5 the third series produced the same growth rate as the two other series (Figure 2. 30); the growth rate was independent of eddy diffusion prior to JD 89.5. This result suggests phytoplankton growth was governed by increasing incident light prior to JD 89.5. Daily-averaged light fluxes were generally increasing up to about JD 100 when the flux decreased (Figure 2. 31). While the post-JD 100 decreasing light levels could have contributed to the decline of the bloom, modeling results show that eddy diffusion has a significant effect on phytoplankton growth (Figure 2. 30).